Scanning electron microscopy with energy dispersive spectroscopy and Raman and infrared spectroscopic study of tilleyite $Ca_5Si_2O_7(CO_3)_2$-Y

Ray L. Frost [a,*], Andrés López [a], Ricardo Scholz [b], Fernando A.N. de Oliveira [c]

[a] School of Chemistry, Physics and Mechanical Engineering, Science and Engineering Faculty, Queensland University of Technology, GPO Box 2434, Brisbane, Queensland 4001, Australia
[b] Geology Department, School of Mines, Federal University of Ouro Preto, Campus Morro do Cruzeiro, Ouro Preto, MG 35,400-00, Brazil
[c] Federal Institute of Minas Gerais, Campus Ouro Preto, Ouro Preto, MG 35,400-000, Brazil

HIGHLIGHTS

- The mineral tilleyite-Y, a carbonate-silicate of calcium, was analysed.
- Using SEM with EDX and vibrational spectroscopy.
- Multiple carbonate stretching modes are observed.
- Supporting the concept of non-equivalent carbonate units.
- Multiple Raman bands in the OH stretching region are observed.

GRAPHICAL ABSTRACT

ARTICLE INFO

ABSTRACT

The mineral tilleyite-Y, a carbonate-silicate of calcium, has been studied by scanning electron microscopy with chemical analysis using energy dispersive spectroscopy (EDX) and Raman and infrared spectroscopy. Multiple carbonate stretching modes are observed and support the concept of non-equivalent carbonate units in the tilleyite structure. Multiple Raman and infrared bands in the OH stretching region are observed, proving the existence of water in different molecular environments in the structure of tilleyite. Vibrational spectroscopy offers new information on the mineral tilleyite.

© 2015 Elsevier B.V. All rights reserved.

Introduction

The mineral tilleyite, a calcium silicate carbonate, with general chemical formula given as $Ca_5Si_2O_7(CO_3)_2$. The mineral was first described from Crestmore quarries, Riverside Co., California, USA [1]. Other occurrences were also reported from Flekkeren, Telemark, Norway [2]; Oravița Skarns, Banat Mts, Caras-Severin Co., Romania [3] and Anakit Creek, Krasnoyarsk Territory, Eastern-Siberian Region, Russia [4,5]. Tilleyite forms in the contact metamorphic zone between igneous rocks and limestones, formed at low pressure and high temperature.

The crystal structure was first determined by Smith [6] and latter refined by Louisnathan and Smith [7] and in recent study by Grice [8]. Tilleyite crystalizes with monoclinic symmetry and the unit cell parameters are: $P21/a$, $a = 15.082(3)$, $b = 10.236(2)$, $c = 7.572(1)$ Å, $\beta = 105.17°$, $V = 1128.3(3)$ Å^3 [7,8]. The structure of tilleyite has [CaO$_8$] polyhedra adjoining [CO$_3$] groups in one layer, whereas [CaO$_8$] polyhedra intertwine [Si$_2$O$_7$] pairs of tetrahedra in the other layer [7,8].

* Corresponding author. Tel.: +61 7 3138 2407; fax: +61 7 3138 1804.
E-mail address: r.frost@qut.edu.au (R.L. Frost).

Spectroscopy of carbonate anion

It is important to understand the vibrational spectroscopy of the carbonate anion in different molecular environments. Nakamoto et al. first published and tabulated the selection rules for unidenate and bidentate anions including the carbonate anion [10,11]. The free ion, CO_3^{2-} with D_{3h} symmetry exhibits four normal vibrational modes; a symmetric stretching vibration (ν_1), an out-of-plane bend (ν_2), a doubly degenerate asymmetric stretch (ν_3) and another doubly degenerate bending mode (ν_4). The symmetries of these modes are A_1' (R) + A_2'' (IR) + E' (R, IR) + E'' (R, IR) and occur at 1063, 879, 1415 and 680 cm^{-1} respectively. Generally, strong Raman modes appear around 1100 cm^{-1} due to the symmetric stretching vibration (ν_1), of the carbonate groups, while intense IR and weak Raman peaks near 1400 cm^{-1} are due to the antisymmetric stretching mode (ν_3). Infrared modes near 800 cm^{-1} are derived from the out-of-plane bend (ν_2). Infrared and Raman modes around 700 cm^{-1} region are due to the in-plane bending mode (ν_4). This mode is doubly degenerate for undistorted CO_3^{2-} groups [11]. As the carbonate groups become distorted from regular planar symmetry, this mode splits into two components [11]. Infrared and Raman spectroscopy provide sensitive test for structural distortion of CO_3^{2-}.

There have been very few studies of mixed anion minerals containing silicate and carbonate. This is the first study of the Raman and infrared spectroscopy of tilleyite. The novelty of this work rests with the application of vibrational spectroscopy to the study of the mineral tilleyite. This type of study is important as new materials based upon the tilleyite structure may be invented. As part of our comprehensive research into minerals containing oxyanions, we report the SEM with EDX and vibrational spectroscopy of tilleyite and related the spectra to the structure of the mineral.

Experimental

Samples description and preparation

The tilleyite sample studied in this work is from Kushiro, Hiba-gun, Hiroshima prefecture, Honshu Island, Japan. The mineral is part in a contact metamorphism paragenesis and occurs in association with vesuvianite and wollastonite.

The compositions have been reported by Anthony et al. (page 192) [9]. The sample was incorporated to the collection of the Geology Department of the Federal University of Ouro Preto, Minas Gerais, Brazil, with sample code SAD-044. The sample was gently crushed and the associated minerals were removed under a stereomicroscope Leica MZ4. Qualitative and semiquantitative chemical analysis via SEM/EDS were applied to the mineral characterization.

Scanning electron microscopy (SEM)

Experiments and analyses involving electron microscopy were performed in the Center of Microscopy of the Universidade Federal de Minas Gerais, Belo Horizonte, Minas Gerais, Brazil (http://www.microscopia.ufmg.br).

Tilleyite crystals were coated with a 5 nm layer of evaporated carbon. Secondary Electron and Backscattering Electron images were obtained using a JEOL JSM-6360LV equipment. Qualitative and semi-quantitative chemical analyses in the EDX mode were performed with a ThermoNORAN spectrometer model Quest and was applied to support the mineral characterization.

Raman microprobe spectroscopy

Crystals of tilleyite were placed on a polished metal surface on the stage of an Olympus BHSM microscope, which is equipped with 10×, 20×, and 50× objectives. The microscope is part of a Renishaw 1000 Raman microscope system, which also includes a monochromator, a filter system and a CCD detector (1024 pixels). The Raman spectra were excited by a Spectra-Physics model 127 He–Ne laser producing highly polarized light at 633 nm and collected at a nominal resolution of 2 cm^{-1} and a precision of ±1 cm^{-1} in the range between 200 and 4000 cm^{-1}. Repeated acquisitions on the crystals using the highest magnification (50×) were accumulated to improve the signal to noise ratio of the spectra. Raman spectra were calibrated using the 520.5 cm^{-1} line of a silicon wafer. The Raman spectrum of at least 10 crystals was collected to ensure the consistency of the spectra.

An image of the tilleyite crystals measured is shown in the Supplementary information as Fig. S1. Clearly the crystals of tilleyite are readily observed, making the Raman spectroscopic measurements readily obtainable.

Infrared spectroscopy

Infrared spectra of tilleyite were obtained using a Nicolet Nexus 870 FTIR spectrometer with a smart endurance single bounce diamond ATR cell. Spectra over the 4000–525 cm^{-1} range were obtained by the co-addition of 128 scans with a resolution of 4 cm^{-1} and a mirror velocity of 0.6329 cm/s. Spectra were co-added to improve the signal to noise ratio.

Spectral manipulation such as baseline correction/adjustment and smoothing were performed using the Spectracalc software package GRAMS (Galactic Industries Corporation, NH, USA). Band component analysis was undertaken using the Jandel 'Peakfit' software package that enabled the type of fitting function to be selected and allows specific parameters to be fixed or varied accordingly. Band fitting was done using a Lorentzian–Gaussian cross-product function with the minimum number of component bands used for the fitting process. The Lorentzian–Gaussian ratio was maintained at values greater than 0.7 and fitting was undertaken until reproducible results were obtained with squared correlations of r^2 greater than 0.995.

Results and discussion

Chemical characterization

The SEM image of tilleyite sample studied in this work is shown in Fig. 1. The image shows a fragment of a single crystal up to 0.5 mm. The fragment shows irregular and conchoidal fractures. The chemical analysis is provided in Fig. 2. The chemical
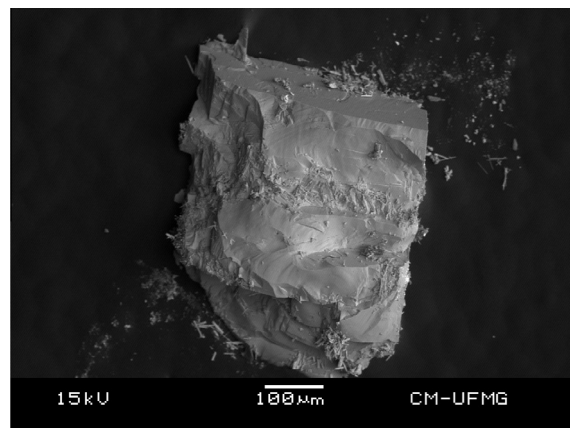

Fig. 1. Backscattered electron image (BSI) of a tilleyite crystal aggregate up to 0.5 mm in length.

composition of the measured mineral sample shows the presence of Ca, C and Si. Minor amounts of Al were also observed.

Vibrational spectroscopy

Vibrational spectroscopy of tilleyite

The Raman spectrum of tilleyite in the 4000–100 cm^{-1} spectral range is displayed in Fig. 3a. This spectrum shows the position and relative intensities of the Raman bands. It is noted that there are
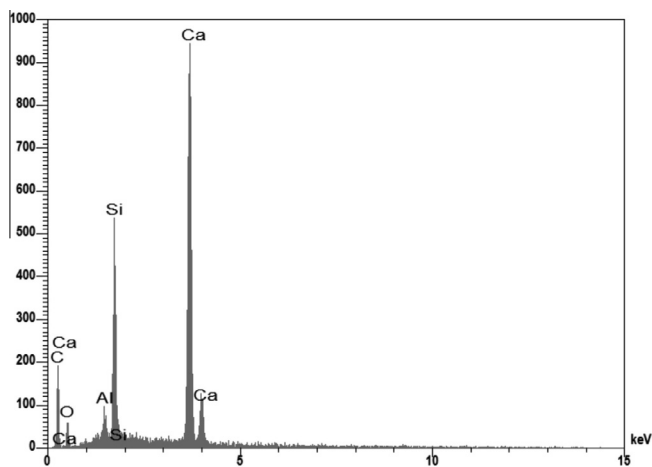

Fig. 2. EDX analysis of tilleyite.

large parts of the spectrum where no intensity or minimal intensity is observed. Thus, the spectrum is subdivided into subsections depending upon the type of vibration being studied. The infrared spectrum of tilleyite in the 4000–500 cm^{-1} spectral region is shown in Fig. 3b. This figure shows the position of the infrared bands and their relative intensities. This spectrum displays the position and relative intensities of the infrared bands. As for the Raman spectrum, there are parts of the spectrum where little or no intensity is observed.

The Raman spectrum of tilleyite over the 1150–950 cm^{-1} spectral range is reported in Fig. 4a. An intense Raman band at 1086 cm^{-1} with shoulder bands at 1080 and 1093 cm^{-1} is assigned to the CO_3^{2-} ν_1 symmetric stretching mode [12–14]. Thus, there appears to be bands attributable to more than one symmetric stretching modes of the carbonate anion. One interpretation of this fact is that there are two distinct non-equivalent carbonate units in the structure of tilleyite. Two broad very low intensity Raman bands at 1047 and 1067 cm^{-1} are attributed to the Si_2O_7 ν_3 antisymmetric stretching mode. Other Raman bands are observed at 986, 999, 1010 and 1018 cm^{-1}. It is thought that some of these bands are due to the Si_2O_7 ν_1 symmetric stretching mode [15–18].

The infrared spectrum of tilleyite over the 1150–650 cm^{-1} spectral range is shown in Fig. 4b. The infrared spectrum is complex to say the least. In this spectrum, there are three distinct spectral features (a) the set of infrared bands centred upon 1060 cm^{-1}, (b) the infrared bands around 873 cm^{-1} and (c) the set of overlapping bands between 650 and 750 cm^{-1}. The infrared bands are quite well resolved. The set of infrared bands at 1020, 1037, 1060, 1080 and 1084 cm^{-1} are assigned to the CO_3^{2-} antisymmetric and symmetric stretching modes [16–18]. The infrared bands at 697,
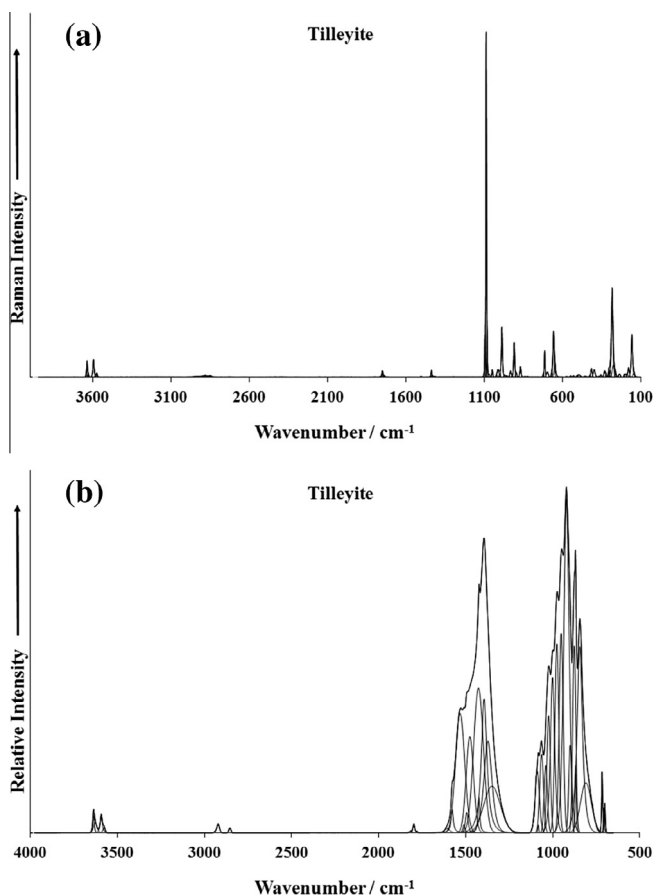

Fig. 3. (a) Raman spectrum of tilleyite over the 100–4000 cm^{-1} spectral range (upper spectrum) (b) Infrared spectrum of tilleyite over the 500–4000 cm^{-1} spectral range (lower spectrum).
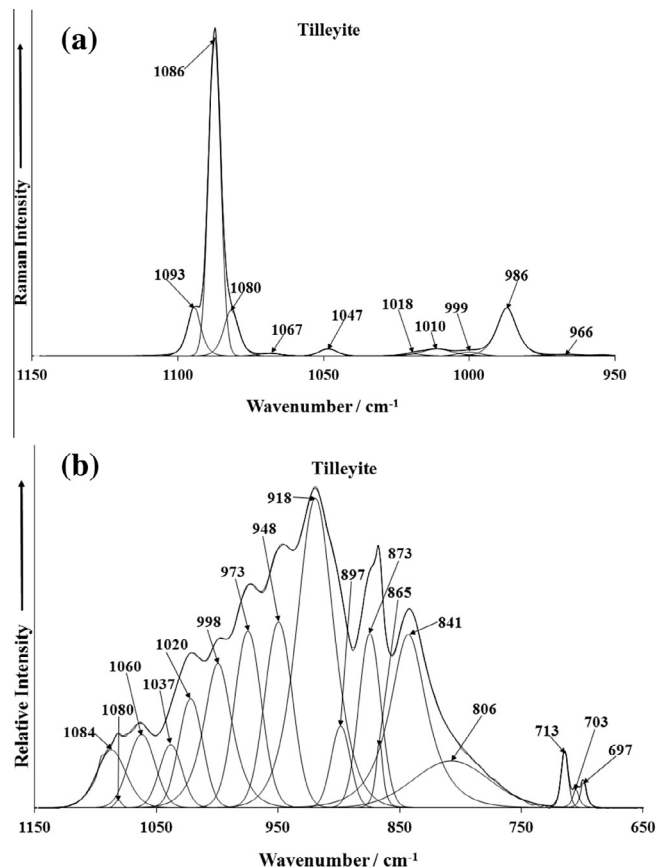

Fig. 4. (a) Raman spectrum of tilleyite (upper spectrum) in the 950–1150 cm^{-1} spectral range and (b) infrared spectrum of tilleyite (lower spectrum) in the 650–1150 cm^{-1} spectral range.

703 and 713 cm^{-1} are assigned to the CO_3^{2-} ν_2 bending modes. The strong infrared bands at 918, 848, 973 and 998 cm^{-1} are considered to be associated with Si_2O_7 antisymmetric and symmetric stretching modes.

The Raman spectrum of tilleyite over the 600–350 cm^{-1} spectral range is reported in Fig. 5a. The Raman bands at 450, 456, 483, 493, 505, 528, 546 and 572 cm^{-1} are assigned to the Si_2O_7 ν_4 bending modes. In the infrared spectrum (Fig. 4b), the series of low intensity bands at 687, 703 and 713 cm^{-1} may also be attributed to this vibrational mode. The series of Raman bands at 589, 611, 674 and 689 cm^{-1} are assigned to the CO_3^{2-} ν_2 bending modes [12–18]. In the Raman spectrum (Fig. 5b), the low intensity bands at 155, 176, 182, 197, 204, 234, 260. 273, 282, 295, 302, 321 and 329 cm^{-1} are attributed to lattice vibrational modes.

The Raman spectrum of tilleyite over the 3700–3500 cm^{-1} spectral range is shown in Fig. 6a. The spectrum shows well resolved Raman bands with well resolved bands at 3574, 3578, 3594, 3629, 3635 and 3638 cm^{-1}. The first two bands at 3574 and 3594 cm^{-1} are assigned to water stretching vibrations. The Raman bands at 3629, 3635 and 3638 cm^{-1} are attributed to the stretching vibrations of hydroxyl units. The observation of bands in the OH stretching region brings into question the actual formula of tilleyite. The Raman spectrum in this spectral region shows the presence of water and OH units in the structure of tilleyite. These observations are confirmed by the bands in the OH stretching region in the infrared spectrum.

The infrared spectrum of tilleyite over the 2800–3800 cm^{-1} spectral range is shown in Fig. 6b. Infrared bands are resolved at 3575, 3590, 3625 and 3635 cm^{-1}. These bands are attributed to
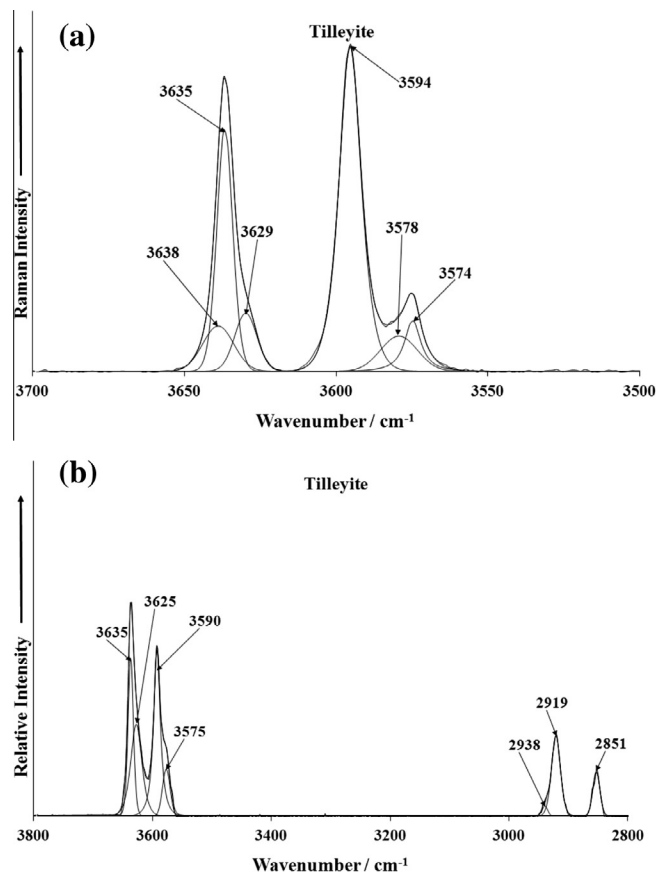

Fig. 6. (a) Raman spectrum of tilleyite (upper spectrum) in the 3500–3700 cm^{-1} spectral range and (b) infrared spectrum of tilleyite (lower spectrum) in the 2800–3800 cm^{-1} spectral range.

water and OH stretching vibrations. The infrared bands at 2851, 2919 and 2938 cm^{-1} are assigned to the stretching vibrations of organic impurities.

The Raman spectrum of tilleyite over the 1800–1400 cm^{-1} spectral range is shown in Fig. 7a. Raman bands are observed at 1412, 1432, 1436, 1442 and 1501 cm^{-1}. These bands are assigned to the CO_3^{2-} ν_3 antisymmetric stretching modes. Intense Raman bands are also noted at 1838, 1748 and 1752 cm^{-1}. The observation of multiple bands in this spectral region is in harmony with the number of Raman bands in the OH stretching region (Fig. 6a). These bands show that water exists in the structure of tilleyite in different molecular environments with differing bond strengths. The infrared spectrum of tilleyite over the 1850–1700 cm^{-1} spectral range is shown in Fig. 7b. Infrared bands are found at 1776, 1795 and 1812 cm^{-1}.

Studies have shown a strong correlation between OH stretching frequencies and both O···O bond distances and H···O hydrogen bond distances [19–24]. [20] showed that a regression function can be employed relating the hydroxyl stretching frequencies with regression coefficients better than 0.96 using infrared spectroscopy [24]. The function is described as: $\nu_1 = (3592 - 304) \times 10^{9^{\frac{-d(O-O)}{0.1321}}}$ cm^{-1}. Thus OH···O hydrogen bond distances may be calculated using the Libowitzky empirical function. The values for the OH stretching vibrations detailed above provide hydrogen bond distances of 0.2735 pm (3279 cm^{-1}), 0.27219 pm (3237 cm^{-1}). Frueh and Golightly suggested some hydrogen bonding exists for tilleyite [24]. The values calculated here, support the concept of strong hydrogen bonding between the OH units and the carbonate anions in the tilleyite structure.
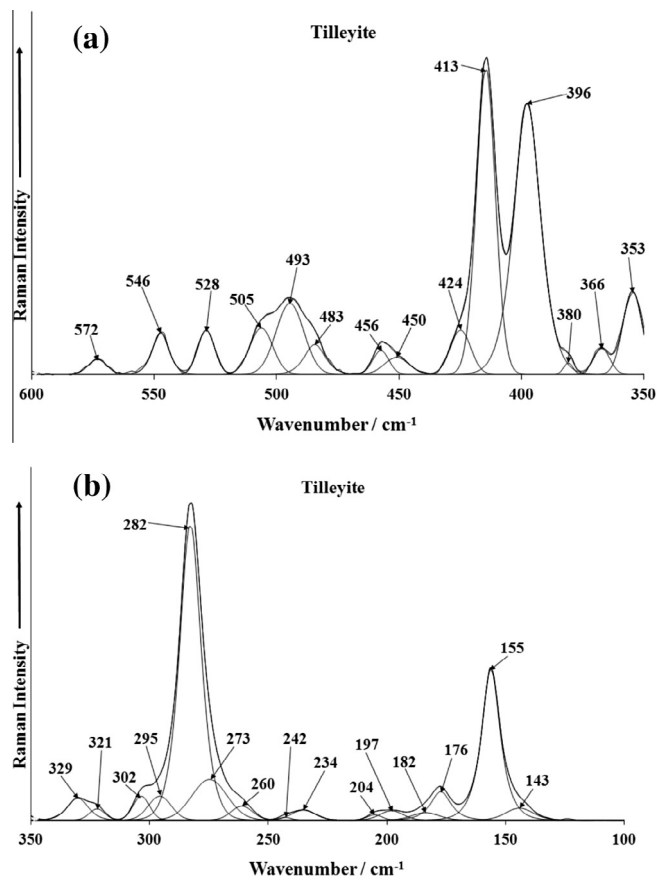

Fig. 5. (a) Raman spectrum of tilleyite (upper spectrum) in the 350–600 cm^{-1} spectral range and (b) Raman spectrum of tilleyite (lower spectrum) in the 100–350 cm^{-1} spectral range.
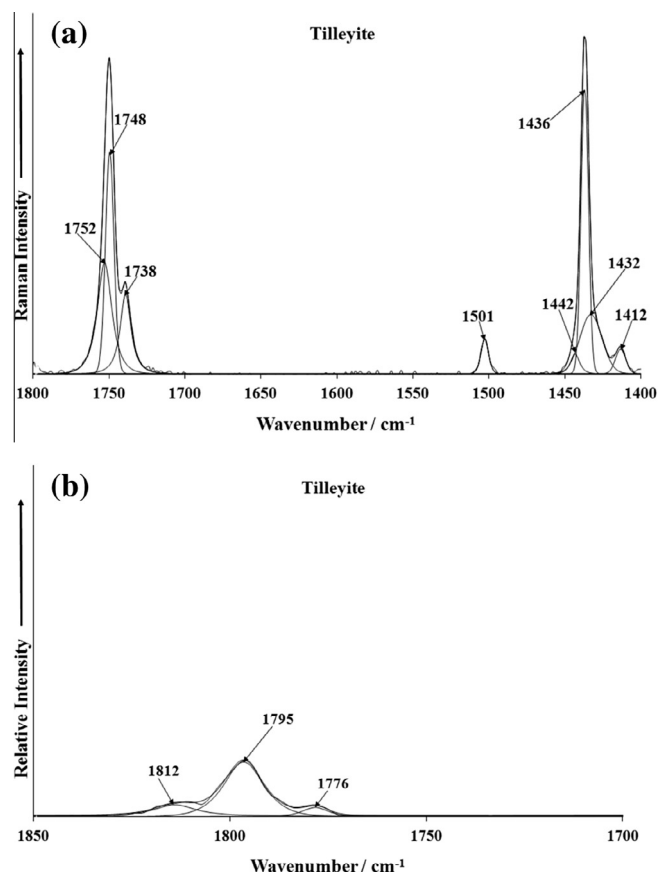
Fig. 7. (a) Raman spectrum of tilleyite (upper spectrum) in the 1400–1800 cm^{-1} spectral range and (b) infrared spectrum of tilleyite (lower spectrum) in the 1700–1850 cm^{-1} spectral range.

Conclusions

The physical properties of the mineral tilleyite have not been forthcoming. In this work the mineral tilleyite from Japan was analysed using a combination of SEM with EDX and vibrational spectroscopy. EDX analysis shows the presence of Ca, C, Si and minor amounts of Al in substitution to Si.

Raman and infrared bands are attributed to the symmetric and antisymmetric stretching modes and bending modes of the CO_3^{2-} and Si_2O_7 units. The mineral tilleyite is characterised by multiple CO_3^{2-} stretching and bending modes, giving credence to the existence of more than one non-equivalent unit in the tilleyite structure. Intense Raman band at 1086 cm^{-1} with shoulder bands at 1080 and 1093 cm^{-1} is assigned to the CO_3^{2-} ν_1 symmetric

stretching mode. Two broad very low intensity Raman bands at 1047 and 1067 cm^{-1} are attributed to the Si_2O_7 ν_3 antisymmetric stretching mode. Raman bands at 765 and 775 cm^{-1} are assigned to the CO_3^{2-} ν_4 bending modes and Raman bands at 589, 611, 674 and 689 cm^{-1} are assigned to the CO_3^{2-} ν_2 bending modes. The Raman and infrared spectrum of tilleyite in the water OH stretching and water bending region shows multiple bands thus providing evidence for the existence of water in the structure of tilleyite in different molecular environments with different hydrogen bond strengths.

Acknowledgements

Appendix A. Supplementary data

Supplementary data associated with this article can be found, in the online version, at http://dx.doi.org/10.1016/j.saa.2015.04.015.

References

[1] E.S. Larsen, K.C. Dunham, Am. Mineral. 18 (1933) 469–473.
[2] B. Jamtveit, S. Dahlgren, H. Austrheim, Am. Mineral. 82 (1997) 1241–1254.
[3] S. Marincea, D.-G. Dumitras, N. Calin, A.M. Anason, A.M. Fransolet, F. Hatert, Can. Mineral. 51 (2013) 359–375.
[4] M.F. Taner, R.F. Martin, R.A. Gault, Can. Mineral. 51 (2013) 893–911.
[5] V.A. Zharikov, D.K. Vlasova, N.N. Pertsev, Tipomorfizm Miner, Ego Prakt. Znachenie, 1972. pp. 194–201.
[6] J.V. Smith, Acta Crystallogr. 6 (1953) 9–18.
[7] S.J. Louisnathan, J.V. Smith, Z. Kristallogr. Kristallgeometrie Kristallphys. Kristallchem. 132 (1970) 288–306.
[8] J.D. Grice, Can. Mineral. 43 (2005) 1489–1500.
[9] J.W. Anthony, R.A. Bideaux, K.W. Bladh, M.C. Nichols, Handbook of Mineralogy, Mineral Data Publishing, Tuscon, Arizona, USA, 2003.
[10] K. Nakamoto, Bunko Kenkyu 5 (1957) 3–13.
[11] K. Nakamoto, J. Fujita, S. Tanaka, M. Kobayashi, J. Am. Chem. Soc. 79 (1957) 4904–4908.
[12] A. Lopez, R.L. Frost, Y. Xi, R. Scholz, Spectrosc. Lett. 47 (2014) 564–570.
[13] R.L. Frost, Y. Xi, R. Scholz, A. Lopez, F.M. Belotti, J. Mol. Struct. 1042 (2013) 1–7.
[14] R.L. Frost, J. Raman Spectrosc. 42 (2011) 1690–1694.
[15] R.L. Frost, B.J. Reddy, S. Bahfenne, J. Graham, Spectrochim. Acta A 72 (2009) 597–604.
[16] R.L. Frost, S. Bahfenne, J. Raman Spectrosc. 40 (2009) 360–365.
[17] R.L. Frost, M.J. Dickfos, J. Cejka, J. Raman Spectrosc. 39 (2008) 582–586.
[18] R.L. Frost, M.J. Dickfos, J. Raman Spectrosc. 38 (2007) 1516–1522.
[19] J. Emsley, Chem. Soc. Rev. 9 (1980) 91–124.
[20] H. Lutz, Struct. Bond. 82 (1995) 85–103.
[21] W. Mikenda, J. Mol. Struct. 147 (1986) 1–15.
[22] A. Novak, Struct. Bond. 18 (1974) 177–216.
[23] E. Libowitsky, Monatsh. Chem. 130 (1999) 1047–1049.
[24] A.J. Frueh Jr., J.P. Golightly, Can. Mineral. 9 (1967) 51–56.